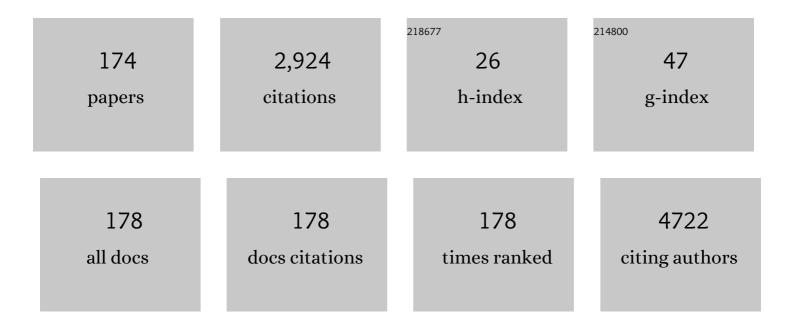
Young Keun Kim

List of Publications by Year in descending order

Source: https://exaly.com/author-pdf/2810766/publications.pdf Version: 2024-02-01



#	Article	IF	CITATIONS
1	Electrical resistivity evolution in electrodeposited Ru and Ru-Co nanowires. Journal of Materials Science and Technology, 2022, 105, 17-25.	10.7	5
2	Engineering the shape of one-dimensional metallic nanostructures via nanopore electrochemistry. Nano Today, 2022, 42, 101348.	11.9	4
3	Variation of spin-orbit torque and spin transport properties by V alloying in β-W-based magnetic heterostructures. Scripta Materialia, 2022, 211, 114486.	5.2	4
4	Surface-ligand-induced crystallographic disorder–order transition in oriented attachment for the tuneable assembly of mesocrystals. Nature Communications, 2022, 13, 1144.	12.8	10
5	Receptor‣evel Proximity and Fastening of Ligands Modulates Stem Cell Differentiation. Advanced Functional Materials, 2022, 32, .	14.9	11
6	Submolecular Ligand Size and Spacing for Cell Adhesion. Advanced Materials, 2022, 34, e2110340.	21.0	13
7	Fluorescent detection of dipicolinic acid as a biomarker in bacterial spores employing terbium ion-coordinated magnetite nanoparticles. Journal of Hazardous Materials, 2021, 408, 124870.	12.4	19
8	Association between Cell Microenvironment Altered by Gold Nanowire Array and Regulation of Partial Epithelialâ€Mesenchymal Transition. Advanced Functional Materials, 2021, 31, 2008758.	14.9	6
9	Highly-sensitive magnetic sensor for detecting magnetic nanoparticles based on magnetic tunnel junctions at a low static field. AIP Advances, 2021, 11, .	1.3	11
10	Remote Switching of Elastic Movement of Decorated Ligand Nanostructures Controls the Adhesionâ€Regulated Polarization of Host Macrophages. Advanced Functional Materials, 2021, 31, 2008698.	14.9	15
11	Remote Control of Timeâ€Regulated Stretching of Ligandâ€Presenting Nanocoils In Situ Regulates the Cyclic Adhesion and Differentiation of Stem Cells. Advanced Materials, 2021, 33, e2008353.	21.0	31
12	Magnetic Nanocoils: Remote Control of Timeâ€Regulated Stretching of Ligandâ€Presenting Nanocoils In Situ Regulates the Cyclic Adhesion and Differentiation of Stem Cells (Adv. Mater. 11/2021). Advanced Materials, 2021, 33, 2170084.	21.0	0
13	Zinc Oxide Nanoâ€6picules on Polylactic Acid for Superâ€Hydrophilic and Bactericidal Surfaces. Advanced Functional Materials, 2021, 31, 2100844.	14.9	11
14	Ruderman–Kittel–Kasuya–Yosida-type interfacial Dzyaloshinskii–Moriya interaction in heavy metal/ferromagnet heterostructures. Nature Communications, 2021, 12, 3280.	12.8	5
15	Immunoregulation of Macrophages by Controlling Winding and Unwinding of Nanohelical Ligands. Advanced Functional Materials, 2021, 31, 2103409.	14.9	19
16	Spin–orbit torque engineering in β-W/CoFeB heterostructures with W–Ta or W–V alloy layers between β-W and CoFeB. NPG Asia Materials, 2021, 13, .	7.9	11
17	Magnetic Control and Realâ€Time Monitoring of Stem Cell Differentiation by the Ligand Nanoassembly. Small, 2021, 17, e2102892.	10.0	22
18	Zinc Oxide Nano‧picules on Polylactic Acid for Superâ€Hydrophilic and Bactericidal Surfaces (Adv.) Tj ETQq0 () 0 rgBT /(Overlock 10 T

#	Article	IF	CITATIONS
19	Inorganic Hollow Nanocoils Fabricated by Controlled Interfacial Reaction and Their Electrocatalytic Properties. Small, 2021, 17, e2103575.	10.0	1
20	Chemical Vapor Synthesis of Nonagglomerated Nickel Nanoparticles by In-Flight Coating. ACS Omega, 2021, 6, 27842-27850.	3.5	7
21	Spin–orbit torques in normal metal/Nb/ferromagnet heterostructures. Scientific Reports, 2021, 11, 21081.	3.3	4
22	Interfacial Perpendicular Magnetic Anisotropy in Magnetic Tunnel Junctions Comprising CoFeB with FeNiSiB Layers. Electronic Materials Letters, 2020, 16, 35-40.	2.2	2
23	Enhancement of perpendicular magnetic anisotropy and Dzyaloshinskii–Moriya interaction in thin ferromagnetic films by atomic-scale modulation of interfaces. NPG Asia Materials, 2020, 12, .	7.9	28
24	Multiâ€Component Mesocrystalline Nanoparticles with Enhanced Photocatalytic Activity. Small, 2020, 16, e2004696.	10.0	9
25	Large and Externally Positioned Ligand-Coated Nanopatches Facilitate the Adhesion-Dependent Regenerative Polarization of Host Macrophages. Nano Letters, 2020, 20, 7272-7280.	9.1	21
26	Independent Tuning of Nanoâ€Ligand Frequency and Sequences Regulates the Adhesion and Differentiation of Stem Cells. Advanced Materials, 2020, 32, 2004300.	21.0	30
27	Nanoâ€Ligands: Independent Tuning of Nanoâ€Ligand Frequency and Sequences Regulates the Adhesion and Differentiation of Stem Cells (Adv. Mater. 40/2020). Advanced Materials, 2020, 32, 2070299.	21.0	0
28	Magnetic Direct-Write Skyrmion Nanolithography. ACS Nano, 2020, 14, 14960-14970.	14.6	17
29	Large reduction in switching current driven by spin-orbit torque in W/CoFeB heterostructures with W–N interfacial layers. Acta Materialia, 2020, 200, 551-558.	7.9	9
30	<i>In Situ</i> Magnetic Control of Macroscale Nanoligand Density Regulates the Adhesion and Differentiation of Stem Cells. Nano Letters, 2020, 20, 4188-4196.	9.1	32
31	Composition-driven crystal structure transformation and magnetic properties of electrodeposited Co–W alloy nanowires. Journal of Alloys and Compounds, 2020, 843, 155902.	5.5	13
32	Heat-Generating Iron Oxide Multigranule Nanoclusters for Enhancing Hyperthermic Efficacy in Tumor Treatment. ACS Applied Materials & Interfaces, 2020, 12, 33483-33491.	8.0	30
33	Strategy to control magnetic coercivity by elucidating crystallization pathway-dependent microstructural evolution of magnetite mesocrystals. Nature Communications, 2020, 11, 298.	12.8	24
34	Thickness and composition-dependent spin-orbit torque behaviors in perpendicularly magnetized Ta/W (t)/CoFeB and Ta1-W /CoFeB junction structures. Journal of Alloys and Compounds, 2020, 823, 153744.	5.5	11
35	Spinâ€Orbit Torque Driven Magnetization Switching and Precession by Manipulating Thickness of CoFeB/W Heterostructures. Advanced Electronic Materials, 2020, 6, 1901004.	5.1	14
36	Design of Magneticâ€Plasmonic Nanoparticle Assemblies via Interface Engineering of Plasmonic Shells for Targeted Cancer Cell Imaging and Separation. Small, 2020, 16, e2001103.	10.0	20

#	Article	IF	CITATIONS
37	Assessment of Cellular Uptake Efficiency According to Multiple Inhibitors of Fe3O4-Au Core-Shell Nanoparticles: Possibility to Control Specific Endocytosis in Colorectal Cancer Cells. Nanoscale Research Letters, 2020, 15, 165.	5.7	7
38	Application of ZnO-Based Nanocomposites for Vaccines and Cancer Immunotherapy. Pharmaceutics, 2019, 11, 493.	4.5	35
39	Metallic Fe–Au Barcode Nanowires as a Simultaneous T Cell Capturing and Cytokine Sensing Platform for Immunoassay at the Single-Cell Level. ACS Applied Materials & Interfaces, 2019, 11, 23901-23908.	8.0	25
40	Properties of a rare earth free L10-FeNi hard magnet developed through annealing of FeNiPC amorphous ribbons. Current Applied Physics, 2019, 19, 599-605.	2.4	10
41	Quantitative Analysis on Cellular Uptake of Clustered Ferrite Magnetic Nanoparticles. Electronic Materials Letters, 2019, 15, 471-480.	2.2	6
42	Application of radially grown ZnO nanowires on poly- <scp>l</scp> -lactide microfibers complexed with a tumor antigen for cancer immunotherapy. Nanoscale, 2019, 11, 4591-4600.	5.6	29
43	Synthesis and Characterization of Magnetic–Luminescent Fe3O4–CdSe Core–Shell Nanocrystals. Electronic Materials Letters, 2019, 15, 102-110.	2.2	11
44	Microwave absorption properties of magnetite multi-granule nanocluster–multiwall carbon nanotube composites. Functional Materials Letters, 2019, 12, 1950011.	1.2	5
45	Formation of high aspect ratio fused silica nanowalls by fluorine-based deep reactive ion etching. Nano Structures Nano Objects, 2018, 15, 212-215.	3.5	5
46	Magnetization reversal of ferromagnetic nanosprings affected by helical shape. Nanoscale, 2018, 10, 20405-20413.	5.6	17
47	Microstructural evolution and electrical resistivity of nanocrystalline W thin films grown by sputtering. Materials Characterization, 2018, 145, 473-478.	4.4	15
48	MnO ₂ Nanowire–CeO ₂ Nanoparticle Composite Catalysts for the Selective Catalytic Reduction of NO <i>_x</i> with NH ₃ . ACS Applied Materials & Interfaces, 2018, 10, 32112-32119.	8.0	32
49	Fabrication of three-dimensional electrical patterns by swollen-off process: An evolution of the lift-off process. Current Applied Physics, 2018, 18, 1235-1239. Role of the Heavy Metal's Crystal Phase in Oscillations of Perpendicular Magnetic Anisotropy and the	2.4	1
50	Interfacial Dzyaloshinskii-Moriya Interaction in <mml:math xmlns:mml="http://www.w3.org/1998/Math/MathML" display="inline"><mml:mrow><mml:mi mathvariant="normal">W<mml:mo>/</mml:mo><mml:mi>Co</mml:mi><mml:mtext>â^'mathvariant="normal">B<mml:mo>/</mml:mo><mml:mi>MgO</mml:mi></mml:mtext></mml:mi </mml:mrow></mml:math 	>< <mark>3:8</mark> ml:mi	>Fe?/mml:mi
51	Films. Physical Review Applied, 2018, 9, Synthesis of Co nanotubes by nanoporous template-assisted electrodeposition via the incorporation of vanadyl ions. Chemical Communications, 2017, 53, 1825-1828.	4.1	10
52	Spontaneous nucleation and topological stabilization of skyrmions in magnetic nanodisks with the interfacial Dzyaloshinskii–Moriya interaction. Journal of Magnetism and Magnetic Materials, 2017, 429, 221-226.	2.3	13
53	Functionalization of 3D printed microâ€containers with Niâ€Au coreâ€shell nanowires. Physica Status Solidi (A) Applications and Materials Science, 2017, 214, 1600887.	1.8	2
54	Annealing effect on the magnetic properties of cobalt-based amorphous alloys. Current Applied Physics, 2017, 17, 548-551.	2.4	6

#	Article	IF	CITATIONS
55	Crystallographic Orientation and Microstructure-Dependent Magnetic Behaviors in Arrays of Ni Nanowires. IEEE Transactions on Magnetics, 2017, 53, 1-4.	2.1	2
56	Synthesis, microstructure, and physical properties of metallic barcode nanowires. Metals and Materials International, 2017, 23, 413-425.	3.4	17
57	Enhancing current-induced torques by abutting additional spin polarizer layer to nonmagnetic metal layer. Scientific Reports, 2017, 7, 45669.	3.3	2
58	Magnetic Particle Spectrometry of Fe ₃ O ₄ Multi-Granule Nanoclusters. IEEE Transactions on Magnetics, 2017, 53, 1-4.	2.1	1
59	Eradication of <i>Plasmodium falciparum</i> from Erythrocytes by Controlled Reactive Oxygen Species via Photodynamic Inactivation Coupled with Photofunctional Nanoparticles. ACS Applied Materials & Interfaces, 2017, 9, 12975-12981.	8.0	7
60	CoFeSiB–Pd multilayers and co-deposited alloy films exhibiting perpendicular magnetic anisotropies after heat treatment up to 500°C. Acta Materialia, 2017, 125, 196-201.	7.9	1
61	Radio frequency-mediated local thermotherapy for destruction of pancreatic tumors using Ni–Au core–shell nanowires. Nanotechnology, 2017, 28, 03LT01.	2.6	13
62	Efficient intracellular delivery of biomacromolecules employing clusters of zinc oxide nanowires. Nanoscale, 2017, 9, 15371-15378.	5.6	24
63	Photonic Reactions Leading to Fluorescence in a Polymeric System Induced by the Photothermal Effect of Magnetite Nanoparticles Using a 780 nm Multiphoton Laser. Small, 2017, 13, 1700897.	10.0	8
64	Magnetically soft FeCoTiZrB alloys with high saturation magnetization. Intermetallics, 2017, 90, 164-168.	3.9	6
65	Effect of the magnetic core size of amino-functionalized Fe 3 O 4 -mesoporous SiO 2 core-shell nanoparticles on the removal of heavy metal ions. Colloids and Surfaces A: Physicochemical and Engineering Aspects, 2017, 531, 133-140.	4.7	67
66	Microstructure and Magnetic Properties of CoFe Nanowires and Helical Nanosprings. IEEE Transactions on Magnetics, 2017, 53, 1-4.	2.1	3
67	Perpendicular Magnetic Anisotropy and Interfacial Dzyaloshinskii-Moriya Interaction in Pt/CoFeSiB Structures. IEEE Magnetics Letters, 2017, 8, 1-4.	1.1	1
68	Magnetization Reversal of Self-Assembled One-Dimensional Chains of Fe304 Nanoparticles. , 2016, , .		0
69	Perpendicular Magnetic Anisotropy of Non-Magnetic Materials/Ferromagnetic Materials/MgO Trilayer. , 2016, , .		0
70	Localized electroporation effect on adherent cells in modified electric cell–substrate impedance sensing circuits. Applied Physics Express, 2016, 9, 107001.	2.4	1
71	Catalytic activity of vanadium oxide catalysts prepared by electrodeposition for the selective catalytic reduction of nitrogen oxides with ammonia. Reaction Kinetics, Mechanisms and Catalysis, 2016, 118, 633-641.	1.7	3
72	Ultrahigh Tensile Strength Nanowires with a Ni/Ni–Au Multilayer Nanocrystalline Structure. Nano Letters, 2016, 16, 3500-3506.	9.1	21

#	Article	IF	CITATIONS
73	White-light-emitting magnetite nanoparticle–polymer composites: photonic reactions of magnetic multi-granule nanoclusters as photothermal agents. Nanoscale, 2016, 8, 17136-17140.	5.6	6
74	Size-dependent changeover in magnetization reversal mode of self-assembled one-dimensional chains of spherical Fe ₃ O ₄ nanoparticles. Japanese Journal of Applied Physics, 2016, 55, 100303.	1.5	5
75	Generation of protective immunity against Orientia tsutsugamushi infection by immunization with a zinc oxide nanoparticle combined with ScaA antigen. Journal of Nanobiotechnology, 2016, 14, 76.	9.1	29
76	Synthesis of Fe Doped ZnO Nanowire Arrays that Detect Formaldehyde Gas. Journal of Nanoscience and Nanotechnology, 2016, 16, 4814-4819.	0.9	4
77	Optimization of Fe/Co ratio in Fe (87-x-y) Co x Ti 7 Zr 6 B y alloys for high saturation magnetization. Current Applied Physics, 2016, 16, 515-519.	2.4	10
78	Effect of Silicon Additions on the Magnetic Properties for Fe-Based Alloys. Journal of Nanoscience and Nanotechnology, 2016, 16, 11210-11213.	0.9	0
79	3 Dimensional-Printed Micro-Container with Graphene Current Collector and Manganese Oxide Thin-Film as Cathodes of Li-Batteries. Nanoscience and Nanotechnology Letters, 2016, 8, 1095-1098.	0.4	0
80	Current fluctuation of electron and hole carriers in multilayer WSe2 field effect transistors. Applied Physics Letters, 2015, 107, .	3.3	12
81	Magnetic multi-granule nanoclusters: A model system that exhibits universal size effect of magnetic coercivity. Scientific Reports, 2015, 5, 12135.	3.3	143
82	The toxicity and distribution of iron oxide–zinc oxide coreâ€shell nanoparticles in C57BL/6 mice after repeated subcutaneous administration. Journal of Applied Toxicology, 2015, 35, 593-602.	2.8	22
83	Functional Manipulation of Dendritic Cells by Photoswitchable Generation of Intracellular Reactive Oxygen Species. ACS Chemical Biology, 2015, 10, 757-765.	3.4	29
84	Fabrication of planar and curved polyimide membranes with a pattern transfer method using ZnO nanowire arrays as templates. Materials Letters, 2015, 149, 109-112.	2.6	7
85	Microstructure and Magnetic Properties of LaSrMnO Nanoparticles and Their Application to Cardiac Immunoassay. IEEE Transactions on Magnetics, 2015, 51, 1-4.	2.1	6
86	Immunochromatographic Assay of Hepatitis B Surface Antigen Using Magnetic Nanoparticles as Signal Materials. IEEE Transactions on Magnetics, 2014, 50, 1-4.	2.1	8
87	Gate-Controlled Spin-Orbit Coupling in InAs/InGaAs Quantum Well Structures. Journal of Nanoscience and Nanotechnology, 2014, 14, 5212-5215.	0.9	3
88	Magnetic Nanodiscs Fabricated from Multilayered Nanowires. Journal of Nanoscience and Nanotechnology, 2014, 14, 7923-7928.	0.9	2
89	Synthesis and magnetic properties of size-tunable MnxFe3â^'xO4 ferrite nanoclusters. Journal of Applied Physics, 2014, 115, 17B517.	2.5	9
90	Effect of compositional variation on the soft magnetic properties ofÂFe(87â^'xâ^'y)CoxTi7 Zr6By amorphous ribbons. Current Applied Physics, 2014, 14, 685-687.	2.4	15

#	Article	IF	CITATIONS
91	Isolation of DNA using magnetic nanoparticles coated with dimercaptosuccinic acid. Analytical Biochemistry, 2014, 447, 114-118.	2.4	60
92	Magnetic Anisotropy Evolution in CoFe/Au Barcode Nanowire Arrays. IEEE Transactions on Magnetics, 2014, 50, 1-4.	2.1	7
93	Phase dependent magnetic properties of Ni–Au alloy nanowires. Materials Letters, 2014, 116, 86-90.	2.6	1
94	Magnetic vortex state and multi-domain pattern in electrodeposited hemispherical nanogranular nickel films. Journal of Magnetism and Magnetic Materials, 2014, 371, 149-156.	2.3	7
95	Self-assembly of fluorescent and magnetic Fe3O4@coordination polymer nanochains. Chemical Communications, 2014, 50, 7617.	4.1	29
96	Efficiency of genomic DNA extraction dependent on the size of magnetic nanoclusters. Journal of Applied Physics, 2014, 115, 178512.	2.5	1
97	Solid-state phase transformation mechanism for formation of magnetic multi-granule nanoclusters. RSC Advances, 2013, 3, 3631.	3.6	32
98	Dynamic Microcontainers as Microvacuums for Collecting Nanomaterials After Clinical Treatments. IEEE Transactions on Magnetics, 2013, 49, 3464-3467.	2.1	1
99	Synthesis, microstructure, and magnetic properties of monosized Mn x Zn y Fe3 â^' x â^' yO4 ferrite nanocrystals. Nanoscale Research Letters, 2013, 8, 530.	5.7	24
100	Tunable synthesis and multifunctionalities of Fe3O4–ZnO hybrid core-shell nanocrystals. Materials Research Bulletin, 2013, 48, 551-558.	5.2	45
101	ZnO–Ag Composite Nanocrystals from Nanoemulsion: Synthesis, Magnetic, and Optical Properties. Applied Physics Express, 2013, 6, 063005.	2.4	1
102	Growth behavior and field emission property of ZnO nanowire arrays on Au and Ag films. AIP Advances, 2013, 3, .	1.3	4
103	Control of Magnetic Domains in Co/Pd Multilayered Nanowires with Perpendicular Magnetic Anisotropy. Journal of Nanoscience and Nanotechnology, 2012, 12, 428-432.	0.9	4
104	Magnetically driven spinning nanowires as effective materials for eradicating living cells. Journal of Applied Physics, 2012, 111, .	2.5	14
105	Morphology and electrical properties of high aspect ratio ZnO nanowires grown by hydrothermal method without repeated batch process. Applied Physics Letters, 2012, 101, 083905.	3.3	14
106	Compositional Dependence of Magnetic Properties in CoFe/Au Nanobarcodes. Applied Physics Express, 2012, 5, 103003.	2.4	18
107	Effects of notch shape on the magnetic domain wall motion in nanowires with in-plane or perpendicular magnetic anisotropy. Journal of Applied Physics, 2012, 111, .	2.5	25
108	One-pot synthesis and characterization of bifunctional Au–Fe3O4 hybrid core–shell nanoparticles. Journal of Alloys and Compounds, 2012, 537, 60-64.	5.5	24

#	Article	IF	CITATIONS
109	Structural and magnetic properties of epitaxial Co2FeAl films grown on MgO substrates for different growth temperatures. Acta Materialia, 2012, 60, 6714-6719.	7.9	18
110	Magnetic NiFe/Au barcode nanowires with self-powered motion. Journal of Applied Physics, 2012, 111, .	2.5	17
111	Magnetic and optical properties of monosized Eu-doped ZnO nanocrystals from nanoemulsion. Journal of Applied Physics, 2012, 111, .	2.5	36
112	Dimensional Dependence of Magnetic Properties in Arrays of CoFe/Au Barcode Nanowire. IEEE Transactions on Magnetics, 2012, 48, 3929-3932.	2.1	9
113	Photosensitizer and vancomycin-conjugated novel multifunctional magnetic particles as photoinactivation agents for selective killing of pathogenic bacteria. Chemical Communications, 2012, 48, 4591.	4.1	74
114	Domain wall configuration and magneto-transport properties in dual spin-valve with nanoconstriction. Applied Physics Letters, 2012, 100, 242409.	3.3	2
115	Magnetic domain wall motion by current injection in CoPt nanowires consisting of notches. Solid State Communications, 2012, 152, 1004-1007.	1.9	1
116	Ni–Au core–shell nanowires: synthesis, microstructures, biofunctionalization, and the toxicological effects on pancreatic cancer cells. Journal of Materials Chemistry, 2011, 21, 12089.	6.7	24
117	Microstructural Changes of Epitaxial Fe/MgO Layers Grown on InAs(001) Substrates. Crystal Growth and Design, 2011, 11, 2889-2896.	3.0	6
118	Effect of interparticle interactions and size dispersion in magnetic nanoparticle assemblies: A static and dynamic study. Applied Physics Letters, 2011, 99, .	3.3	21
119	Nonaqueous synthesis and magnetic properties of ZnFe2O4 nanocrystals with narrow size distributions. Journal of Applied Physics, 2011, 109, 07B511.	2.5	11
120	Non-aqueous synthesis of water-dispersible Fe ₃ O ₄ –Ca ₃ (PO ₄) ₂ core–shell nanoparticles. Nanotechnology, 2011, 22, 055701.	2.6	13
121	A multifunctional core–shell nanoparticle for dendritic cell-based cancer immunotherapy. Nature Nanotechnology, 2011, 6, 675-682.	31.5	470
122	Effects of Co addition on magneto-transport properties of magnetic tunnel junction consisting of CoFeB or CoFeSiB free layer. Journal of Applied Physics, 2011, 109, 07D346.	2.5	4
123	Tocopheryl oligochitosan-based self assembling oligomersomes for siRNA delivery. Biomaterials, 2011, 32, 849-857.	11.4	50
124	Fabrication and characterization of RF nanoantenna on a nanoliter-scale 3D microcontainer. Nanotechnology, 2011, 22, 455303.	2.6	5
125	Labeling of macrophage cell using biocompatible magnetic nanoparticles. Journal of Applied Physics, 2011, 109, 07B309.	2.5	9
126	Observation of Suppressed Interdiffusion in FeRh/FePt-Ta Bilayer Thin Films. IEEE Transactions on Magnetics, 2010, 46, 2104-2107.	2.1	1

#	Article	IF	CITATIONS
127	Self-assembly of iron oxide nanoparticles mediated by phospholipids. , 2010, , .		0
128	Spin wave quantization in continuous film with stripe domains. Journal of Applied Physics, 2009, 105, 07D544.	2.5	10
129	Transport Properties of Magnetic Tunnel Junctions Comprising NiFeSiB/CoFeB Hybrid Free Layers. IEEE Transactions on Magnetics, 2009, 45, 2364-2366.	2.1	4
130	Giant Diamagnetism in AuFe Nanoparticles. IEEE Transactions on Magnetics, 2009, 45, 2442-2445.	2.1	5
131	Synthesis and Magnetic Properties of Multifunctional Fe\$_{3}\$O\$_{4}\$-AuPt Core-Shell Nanoparticles. IEEE Transactions on Magnetics, 2009, 45, 4041-4044.	2.1	5
132	A highly sensitive and selective diagnostic assay based on virus nanoparticles. Nature Nanotechnology, 2009, 4, 259-264.	31.5	158
133	Synthesis and magnetic properties of multifunctional CoPtAu nanoparticles. Journal of Applied Physics, 2009, 105, 07B527.	2.5	3
134	Fabrication of Multifunctional Au Doped CoPt Nanowires. IEEE Transactions on Magnetics, 2009, 45, 2471-2474.	2.1	5
135	Synthesis of streptavidin-FITC-conjugated core–shell Fe3O4-Au nanocrystals and their application for the purification of CD4+ lymphocytes. Biomaterials, 2008, 29, 4003-4011.	11.4	99
136	Synthesis and Characterization of \${m Fe-FeO}_{m x}\$ Core-Shell Nanowires. IEEE Transactions on Magnetics, 2008, 44, 3950-3953.	2.1	12
137	Structural and Magnetic Properties of Amorphous and Nanocrystalline CoFeSiB Thin Films. IEEE Nanotechnology Magazine, 2008, 7, 409-411.	2.0	4
138	Magneto-Transport Characteristics of Magnetic Tunnel Junction With a Synthetic Antiferromagnetic Amorphous CoFeSiB Free Layer. IEEE Transactions on Magnetics, 2008, 44, 2598-2600.	2.1	0
139	Growth and Magnetic Properties of CoPtAu Nanowires. IEEE Transactions on Magnetics, 2008, 44, 2726-2729.	2.1	1
140	Magnetoresistance Variation of Magnetic Tunnel Junctions with NiFeSiB/CoFeB Free Layers Depending on MgO Tunnel Barrier Thickness. IEEE Transactions on Magnetics, 2008, 44, 2547-2550.	2.1	6
141	Iron–Gold Barcode Nanowires. Angewandte Chemie - International Edition, 2007, 46, 3663-3667.	13.8	94
142	Electrochemical preparation of Co ₃ Pt nanowires. Physica Status Solidi (A) Applications and Materials Science, 2007, 204, 4158-4161.	1.8	5
143	Synthesis and microwave properties of highly permeable FeCoâ€based nanoâ€alloys. Physica Status Solidi (A) Applications and Materials Science, 2007, 204, 4087-4090.	1.8	11
144	High-frequency noise absorbing properties of nickel nanowire arrays prepared by DC electrodeposition. Physica Status Solidi (A) Applications and Materials Science, 2007, 204, 4025-4028.	1.8	4

#	Article	IF	CITATIONS
145	Magnetotransport of lateral Py/Pt/Py spin valve device. Physica Status Solidi (B): Basic Research, 2007, 244, 4534-4537.	1.5	0
146	Fabrication of suspended single-walled carbon nanotubesvia a direct lithographic route. Journal of Materials Chemistry, 2006, 16, 174-178.	6.7	8
147	Structural and magnetic properties of amorphous and nanocrystalline CoFeSiB thin films. , 2006, , .		Ο
148	Experimental and Simulation Study to Identify Current-Confined Path in Cu–Al Space Layer for CPP-GMR Spin-Valve Applications. IEEE Transactions on Magnetics, 2006, 42, 2633-2635.	2.1	3
149	Switching behavior of indium selenide-based phase-change memory cell. IEEE Transactions on Magnetics, 2005, 41, 1034-1036.	2.1	53
150	Influence of freelayer in magnetic tunnel junction on switching of submicrometer magnetoresistive random access memory arrays. IEEE Transactions on Magnetics, 2005, 41, 883-886.	2.1	5
151	The pH dependence of Co-Cu alloy thin films fabricated on amorphous substrate by DC electrodeposition. IEEE Transactions on Magnetics, 2005, 41, 930-932.	2.1	14
152	Control of magnetic behavior in Fe/sub 3/O/sub 4/ nanostructures. IEEE Transactions on Magnetics, 2005, 41, 3304-3306.	2.1	5
153	Switching characteristics of magnetic tunnel junctions with a synthetic antiferromagnetic free layer. IEEE Transactions on Magnetics, 2005, 41, 2688-2690.	2.1	0
154	Magnetization switching and tunneling magnetoresistance effects with synthetic antiferromagnet free layers consisting of amorphous CoFeSiB. , 2005, , .		0
155	Switching characteristics in magnetic tunnel junctions with a synthetic antiferromagentic free layer. , 2005, , .		0
156	Magnetic properties of Fe/sub 3/O/sub 4/ nanostructures. , 2005, , .		0
157	Current aspects and future perspectives of high-density MRAM. Physica Status Solidi A, 2004, 201, 1617-1620.	1.7	5
158	Magnetic tunnel junctions stabilized by modified synthetic antiferromagnets. Physica Status Solidi A, 2004, 201, 1676-1679.	1.7	2
159	Soft magnetic properties of sub 10 nm NiFe and Co films encapsulated with Ta or Cu. Physica Status Solidi A, 2004, 201, 1859-1861.	1.7	1
160	Optimization of Ru intermediate layer in CoCr-based perpendicular magnetic recording media. Physica Status Solidi A, 2004, 201, 1763-1766.	1.7	10
161	Effect of plasma oxidation time and annealing condition on the temperature dependence of tunneling magnetoresistance. Metals and Materials International, 2003, 9, 57-59.	3.4	1
162	Analysis on giant magnetoresistive characteristics of synthetic antiferromagnet-based spin valves with modified pinned layers. IEEE Transactions on Magnetics, 2003, 39, 2399-2401.	2.1	1

#	Article	IF	CITATIONS
163	Effect of Zr concentration on the microstructure of Al and the magnetoresistance properties of the magnetic tunnel junction with a Zr-alloyed Al–oxide barrier. Applied Physics Letters, 2003, 83, 317-319.	3.3	33
164	Thermal and Mn diffusion behaviors of CoNbZr-based spin valves with nano oxide layers. IEEE Transactions on Magnetics, 2003, 39, 2824-2826.	2.1	3
165	Characteristics of magnetic tunnel junctions consisting of amorphous CoNbZr layers. Journal of Applied Physics, 2003, 93, 8361-8363.	2.5	10
166	Thermal stability of spin-valves incorporating amorphous CoNbZr under and capping layers. Journal of Applied Physics, 2002, 91, 8581.	2.5	25
167	Interlayer diffusion and specularity aspects of amorphous CoNbZr-based spin-valves. IEEE Transactions on Magnetics, 2002, 38, 2685-2687.	2.1	11
168	MR characteristics of synthetic ferrimagnet based spin-valves with different pinning layer thickness ratios. IEEE Transactions on Magnetics, 2000, 36, 2857-2859.	2.1	0
169	Design of recessed yoke heads for minimizing adjacent track encroachment. IEEE Transactions on Magnetics, 2000, 36, 2524-2526.	2.1	8
170	Structural and magnetoresistance characteristics of CoFe/Ag/NiFe/Ag composite discontinuous multilayers. Applied Physics Letters, 2000, 77, 4199-4201.	3.3	1
171	Exchange anisotropy and thermal stability of Mn-Ir-Pt exchange-biased layers. IEEE Transactions on Magnetics, 2000, 36, 2569-2571.	2.1	2
172	Interface Electronic And Magnetic Structures Of Layered Fe In Contact With MgO. Materials Research Society Symposia Proceedings, 1991, 238, 799.	0.1	0
173	Thermal and Mn diffusion behaviors of CoNbZr based spin valves with nano-oxide layers. , 0, , .		0
174	Spin-orbit torque efficiency in Ta or W/Ta-W/CoFeB junctions. Materials Research Express, 0, , .	1.6	0